

# Coherent ecological dynamics induced by large-scale disturbance

Timothy H. Keitt<sup>1</sup>

Aggregate community-level response to disturbance is a principle concern in ecology because post-disturbance dynamics are integral to the ability of ecosystems to maintain function in an uncertain world. Community-level responses to disturbance can be arrayed along a spectrum ranging from synchronous oscillations where all species rise and fall together, to compensatory dynamics where total biomass remains relatively constant despite fluctuations in the densities of individual species<sup>1</sup>. An important recent insight is that patterns of synchrony and compensation can vary with the timescale of analysis<sup>2</sup> and that spectral time series methods can enable detection of coherent dynamics that would otherwise be obscured by opposing patterns occurring at different scales<sup>3</sup>. Here I show that application of wavelet analysis to experimentally manipulated plankton communities reveals strong synchrony after disturbance. The result is paradoxical because it is well established that these communities contain both disturbance-sensitive and disturbance-tolerant species leading to compensation within functional groups<sup>4,5</sup>. Theory predicts that compensatory substitution of functionally equivalent species should stabilize ecological communities<sup>6–10</sup>, yet I found at the whole-community level a large increase in seasonal biomass variation. Resolution of the paradox hinges on patterns of seasonality among species. The compensatory shift in community composition after disturbance resulted in a loss of cold-season dominants, which before disturbance had served to stabilize biomass throughout the year. Species dominating the disturbed community peaked coherently during the warm season, explaining the observed synchrony and increase in seasonal biomass variation. These results suggest that theory relating compensatory dynamics to ecological stability needs to consider not only complementarity in species responses to environmental change, but also seasonal complementarity among disturbance-tolerant and disturbance-sensitive species.

I analysed time series data of 10 dominant zooplankton species sampled over a 17-year period from Little Rock Lake (LRL), Wisconsin, United States (LRL zooplankton data, North Temperate Lakes Long-Term Ecological Research programme). Only crustaceans were included; however, these have been shown to dominate zooplankton biomass in this system<sup>5</sup>. The experimental treatment effect was applied as a transient 'press' perturbation: the lake was separated into two basins at the beginning of the study and pH was artificially reduced in one of the basins from 1985 to 1990, after which the basins remained separated and pH was allowed to return to baseline conditions<sup>11</sup>. Laboratory assays indicate variation among LRL zooplankton species in their tolerance to acidification; it is well established that interactions between these species form a complex web of positive and negative effects<sup>4,5</sup>. The consequences of these complex interactions for community-level variation have remained enigmatic as we have previously lacked methods

sufficiently sensitive to isolate clear evidence for whole-community synchrony or compensation across multiple scales.

Using a multivariate wavelet analysis (see Methods), I found a marked contrast in community dynamics between reference and treatment basins (Fig. 1). The reference basin had a weak trend towards synchrony at sub-annual timescales and a trend towards compensation at annual and longer scales. Short bursts of both synchronous and compensatory dynamics were observed within the reference basin. Some caution is warranted, however, in interpreting short runs of significant values as they often represent false positives<sup>12</sup>. In contrast, the treatment basin exhibited a powerful synchronous annual-scale signal throughout the period of pH reduction and over much of the recovery period. Notably, the pattern of synchrony appears at the beginning of the time series before separation of the basins. Although this observation might suggest latent difference between the basins unrelated to disturbance, I believe this conclusion is unwarranted for several reasons. First, there is an intrinsic limitation in how precisely wavelet results can be localized in time<sup>13</sup> and therefore results at the initial boundary necessarily contain information from subsequent years that were subject to the treatment effect. Second, results near the beginning and end of the time series can be influenced by truncation of the wavelet and so should be interpreted with caution. Third, statistically significant differences in modulus ratios between basins only appear much later in the time series data (Fig. 2), indicating that differences between basins during the first several years were slight. During the period when modulus ratios were significantly different between basins, the treatment basin showed marked changes in seasonal biomass dynamics (Fig. 2). Wavelet analysis of biomass summed across species shows that synchrony in the treatment basin resulted in a greater than fourfold increase in total annual-scale biomass variation. The increase in biomass variation was also apparent in the raw untransformed time series data: the median absolute deviations of total biomass in the reference and treatment basins were 77.4 and 106.9  $\mu\text{g l}^{-1}$ , respectively. Increased biomass variation was furthermore associated with a nearly two-month phase shift in the timing of annual peak biomass between the two basins.

The strong phase shift in total biomass suggests alteration of species phase relationships (Fig. 3 and Supplementary Fig. 1). Individual phase relationships can be examined by plotting the wavelet coefficients as vectors in the complex plane (Fig. 3). Vector pairs pointing in the same direction indicate perfect synchrony between species; those in the opposite direction, perfect compensation. Vector lengths (here log-transformed to aid visualization) scale with the difference between minimum and maximum biomass during the year. During the period of maximal difference in modulus ratio between basins, phases in the reference basin were spread relatively evenly across seasons ( $P > 0.05$ ; Rao's spacing test<sup>14</sup>;  $H_0$  = angular uniformity). Phases in the treatment basin were strongly clustered

<sup>1</sup>Integrative Biology, University of Texas, Austin, Texas 78712, USA.

( $P < 0.01$ ; Rao's spacing test). A test of equivalence in mean direction and angular dispersion between basins was negative ( $P = 0.46$  and  $P = 0.22$ ; Rao's two-sample test). Notice the strong phase shift and increase in the length of the total biomass vector in the treatment basin (Fig. 3). Although most species showed some difference in phase and amplitude between basins, the most significant impact on total biomass variation was the marked reduction in amplitude of two acid-sensitive species: *Leptodiaptomus minutus*, a herbivorous copepod, and *Diacyclops thomasi*, a predatory copepod. Both of these species reach high abundances during winter months in the reference basin, serving to counterbalance the group of summer-peaking species (see also Supplementary Fig. 1). The outcome of this counterbalance effect was to reduce seasonal biomass variation in the reference basin. Near absence of these winter dominant species in the treatment basin caused an overall reduction in total biomass and a marked increase in seasonal biomass variation. The net effect of all these changes was strongly synchronous dynamics in the disturbed system.

Although previous studies have found evidence of synchrony between individual species pairs in these data<sup>2,4</sup>, to my knowledge this is the first study to demonstrate conclusively that compensatory

shifts can lead to whole-community synchrony after disturbance. Notably, the observed synchrony is directly related to an increase in temporal variability of total community biomass, a clear indication of changed ecological function despite compensatory maintenance of biomass within functional groups. One may legitimately question how general these results are. There is of course a lack of treatment replication, a problem inherent in large-scale ecological experiments. A recent meta-analysis of published community data sets suggested that positive temporal covariance within communities may be more common than negative covariance<sup>15</sup>. The study only reported frequencies of the occurrence of positive and negative values and did not attempt to assert whether any of the observed covariances are larger or smaller than would be expected by chance alone. Nonetheless, the conclusion that communities can experience net positive covariance owing to external forces like seasonality is consistent with the general conclusions of this study. It is notable that the reference basin in this study showed a marginally significant trend towards compensation during some phases of the experiment, demonstrating that nonrandom negative covariance does occur under baseline conditions in at least one case.

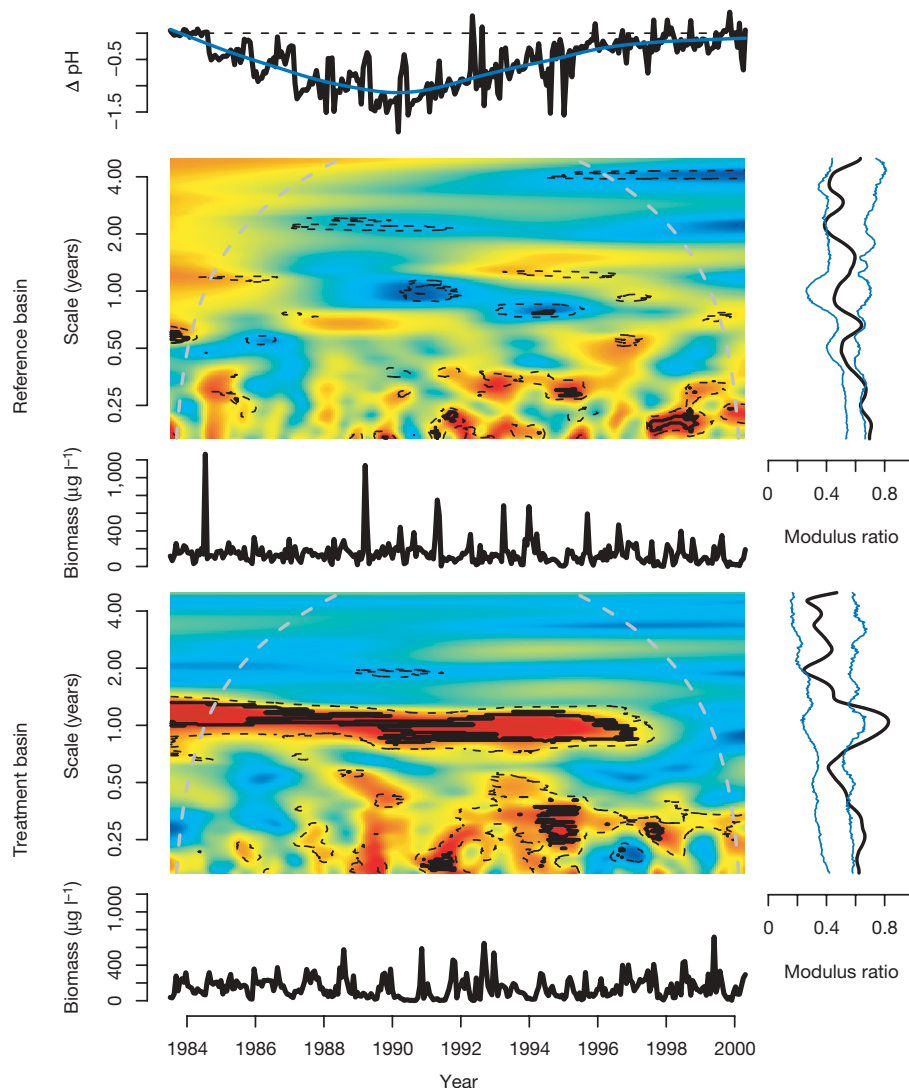


**Figure 1 | Wavelet modulus ratio for reference and treatment basins.** The top inset shows the difference in pH between the basins. The trend line is a smooth spline fit. Heat maps show the modulus ratio scaled from 0 (dark blue denotes compensation) to 1 (dark red represents synchrony). Thin dashed lines delineate regions where the modulus ratio fell outside phase-perturbed 95% confidence intervals (see Methods). Heavy solid lines indicate regions significantly different from the null model with the false

discovery rate controlled at the 5% level. The dashed grey lines indicate  $\pm 1$  unit of scale (or equivalently  $\pm 1$  cycle) from boundaries. Values nearer the boundaries should be interpreted with caution. Inset time series show biomass summed across the ten species. The right margin plots show the global modulus ratio (see Methods) with phase-perturbed 95% confidence intervals.

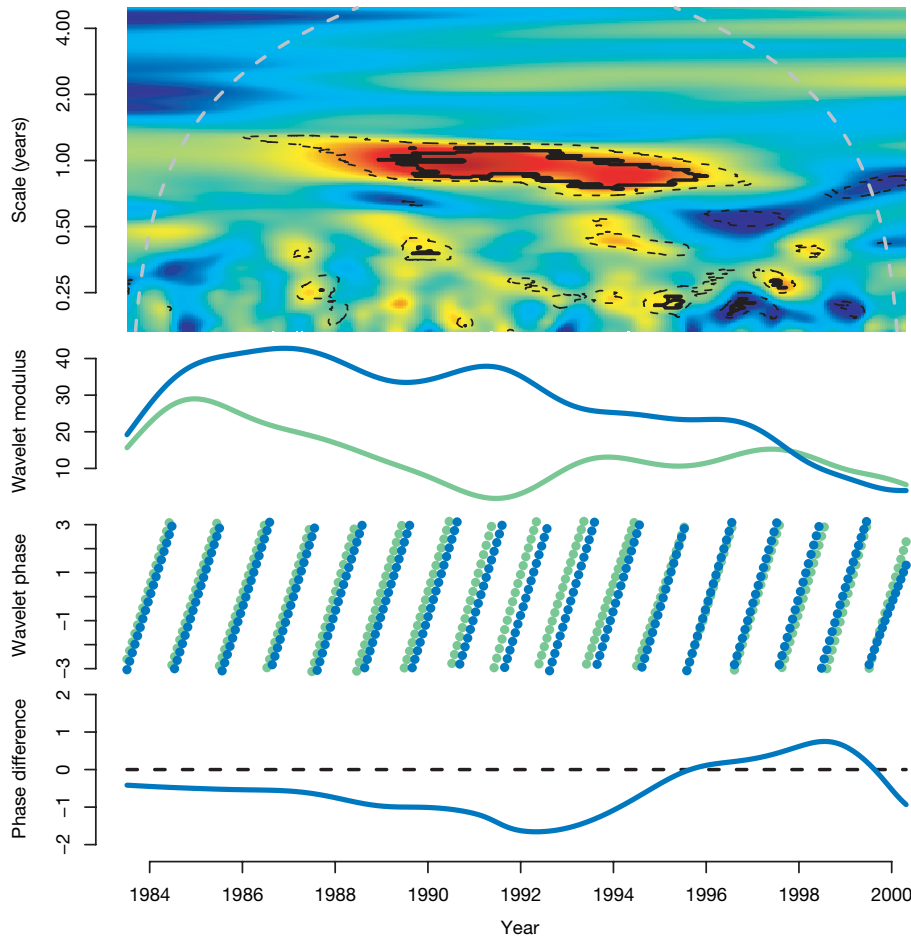


**Figure 2 | Modulus ratio difference between basins.** The heat map shows the difference between the basins (contours as in Fig. 1). Wavelet moduli (blue represents reduced pH; green symbolizes reference) were computed on the time series of summed biomass; larger values indicate greater summed biomass variation. Phase angles and phase difference were also computed from summed biomass.

Mechanisms explaining synchronous or compensatory dynamics in response to disturbance depend crucially on the timing, magnitude and type of disturbance. The disturbance in this study was administered as a sustained reduction in pH, but disturbances can also come as single shocks or periodic fluctuations. The results might have been quite different with periodic disturbance. The simplest explanation for community synchrony is if all species respond identically to periodic disturbance<sup>16,17</sup>. However, it seems likely that cascading ecological interactions in complex communities<sup>18–20</sup> could easily override simple linear effects. For example, a recent modelling study suggested that periodic disturbance can induce synchrony in previously asynchronous communities by disrupting lagged resource–consumer cycles<sup>21</sup>. Interestingly, the synchrony in these models was associated with a reduction in overall biomass variation, the opposite of results presented here. Another recent study showed that periodic nutrient pulsing caused an overall reduction in synchrony and a decrease in biomass variability in experimentally manipulated communities<sup>22</sup>, suggesting that periodic inputs can disrupt endogenous cycles and reduce temporal biomass variation. The candidate mechanism at work in this study was entirely different as species responded to a sustained change in environmental conditions rather than periodic disturbance. Seasonality is an important factor affecting community dynamics in the LRL ecosystem. However, seasonality alone was not sufficient to generate coherent dynamics as annual-scale synchrony was not present in the reference basin. Variation in species responses to reduced pH resulted in strong seasonal clustering and synchrony in the treatment basin. These results suggest that current theory needs to become more attuned to potential interactions between environmental change, seasonality and internal community dynamics in order to provide more accurate predictions of community-level response to large-scale disturbance. Further development of time-frequency methods for community

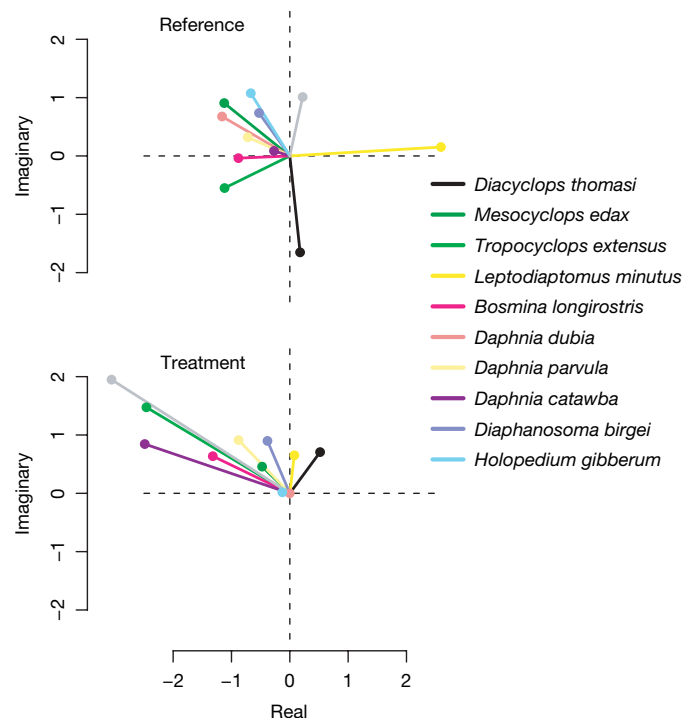


**Figure 3 | Snapshot of species phase relationships at the 1-year timescale.** Wavelets were centred on 10 October 1990, the approximate date of maximum difference in wavelet modulus ratio between basins (see heat map at the top of Fig. 2). Contribution of data values preceding and following the central date decay by 63% per year. Vector lengths correspond to the log-transformed modulus of each species. Vector orientations indicate species phases computed at the annual timescale. The grey vectors give the same results, but for total biomasses rather than individual species.

analysis would be welcome, as would the development of new models that can account for transient synchrony arising through complex interaction between seasonality, disturbance and population dynamics.

## METHODS SUMMARY

I used the continuous wavelet transform<sup>13,23–25</sup>

$$w_k(t, s) = s^{-1} \int_{-\infty}^{\infty} \psi\left(\frac{t-\tau}{s}\right) x_k(\tau) d\tau \quad (1)$$

to detect synchronous and compensatory community dynamics. Here,  $s$  sets the scale of analysis,  $\psi(\tau)$  is the wavelet function and  $x_k(\tau)$  is the biomass of the  $k$ th species at time  $\tau$ . I used the complex-valued Morlet wavelet<sup>26</sup>  $\psi(\tau) = \pi^{-1/4} \exp(2\pi i\tau - \frac{1}{2}\tau^2)$  in all analyses. Coherency was measured using the localized wavelet modulus ratio

$$\rho(t, s) = \frac{A_{t,s}(|\sum_k w_k(\tau, s)|)}{A_{t,s}(\sum_k |w_k(\tau, s)|)} \quad (2)$$

where  $A_{t,s}(\cdot) = \int_{-\infty}^{\infty} e^{-\frac{1}{2}(\frac{t-\tau}{s})^2} (\cdot) d\tau$  and  $|\cdot|$  denotes the modulus or complex norm. The numerator of equation (2) quantifies aggregate biomass variation at time  $t$  and scale  $s$ , whereas the denominator captures individual species variation. Under compensatory dynamics, aggregate variation is small relative to individual species variation and the modulus ratio tends towards zero. With synchrony, aggregate variation approaches the sum of individual species variation and the modulus ratio tends towards one.

**Full Methods** and any associated references are available in the online version of the paper at [www.nature.com/nature](http://www.nature.com/nature).

**Received 5 March; accepted 25 March 2008.**

1. Micheli, F. *et al.* The dual nature of community variability. *Oikos* **85**, 161–169 (1999).
2. Keitt, T. H. & Fischer, J. Detection of scale-specific community dynamics using wavelets. *Ecology* **87**, 2895–2904 (2006).
3. Vasseur, D. A. & Gaedke, U. Spectral analysis unmasks synchronous and compensatory dynamics in plankton communities. *Ecology* **88**, 2058–2071 (2007).
4. Fischer, J. M., Frost, T. M. & Ives, A. R. Compensatory dynamics in zooplankton community responses to acidification: Measurement and mechanisms. *Ecol. Appl.* **11**, 1060–1072 (2001).
5. Frost, T. M., Fischer, J. M., Klug, J. L., Arnott, S. E. & Montz, P. K. Trajectories of zooplankton recovery in the Little Rock Lake whole-lake acidification experiment. *Ecol. Appl.* **16**, 353–367 (2006).
6. Tilman, D. The ecological consequences of changes in biodiversity: a search for general principles. *Ecology* **80**, 1455–1474 (1999).
7. McCann, K. S. The diversity-stability debate. *Nature* **405**, 228–233 (2000).

8. Cottingham, K. L., Brown, B. L. & Lennon, J. T. Biodiversity may regulate the temporal variability of ecological system. *Ecol. Lett.* **4**, 72–85 (2001).
9. Loreau, M. *et al.* Ecology - Biodiversity and ecosystem functioning: Current knowledge and future challenges. *Science* **294**, 804–808 (2001).
10. Hooper, D. U. *et al.* Effects of biodiversity on ecosystem functioning: A consensus of current knowledge. *Ecol. Monogr.* **75**, 3–35 (2005).
11. Forst, T. M. *et al.* The experimental acidification of Little Rock Lake. In *Long-Term Dynamics of Lakes in the Landscape* (eds Magnuson, J. J., Kratz, T. K. & Benson, B. J.) (Oxford Univ. Press, New York, 2005).
12. Maraun, D. & Kurths, J. Cross wavelet analysis: significance testing and pitfalls. *Nonlin. Processes Geophys.* **11**, 505–514 (2004).
13. Daubechies, I. *Ten Lectures On Wavelets*. CBMS-NSF Regional Conference Series in Applied Mathematics (Society for Industrial and Applied Mathematics, Philadelphia, 1992).
14. Rao, J. S. & SenGupta, A. *Topics in Circular Statistics* (World Scientific, Singapore, 2001).
15. Houlihan, J. E. *et al.* Compensatory dynamics are rare in natural ecological communities. *Proc. Natl Acad. Sci. USA* **104**, 3273–3237 (2007).
16. Moran, P. A. P. The statistical analysis of the Canadian lynx cycle. II. synchronization and meteorology. *Aust. J. Zool.* **1**, 291–298 (1953).
17. Kent, A. D., Yannarell, A. C., Rusak, J. A., Triplett, E. W. & McMahon, K. D. Synchrony in aquatic microbial community dynamics. *ISME J.* **1**, 38–47 (2007).
18. Carpenter, S. R., Kitchell, J. F. & Hodgson, J. R. Cascading trophic interactions and lake productivity. *Bioscience* **35**, 634–639 (1985).
19. Ives, A. R. Predicting the response of populations to environmental change. *Ecology* **76**, 926–941 (1995).
20. Pace, M. L., Cole, J. J., Carpenter, S. R. & Kitchell, J. F. Trophic cascades revealed in diverse ecosystems. *Trends Ecol. Evol.* **14**, 483–488 (1999).
21. Vasseur, D. A. & Fox, J. W. Environmental fluctuations can stabilize food web dynamics by increasing synchrony. *Ecol. Lett.* **10**, 1066–1074 (2007).
22. Downing, A. L., Brown, B. L., Perrin, E. M., Keitt, T. H. & Leibold, M. A. Environmental fluctuations induce scale-dependent compensation and increase stability in plankton ecosystems. *Ecology* (in the press).
23. Mallat, S. *A Wavelet Tour of Signal Processing* 2nd edn (Academic, New York, 1999).
24. Grenfell, B. T., Bjornstad, O. N. & Kappey, J. Travelling waves and spatial hierarchies in measles epidemics. *Nature* **414**, 716–723 (2001).
25. Percival, D. B. & Walden, A. T. *Wavelet Methods in Time Series Analysis*. Cambridge Series in Statistical and Probabilistic Mathematics (Cambridge Univ. Press, Cambridge, UK, 2002).
26. Grossmann, A. & Morlet, J. Decomposition of Hardy functions into square integrable wavelets of constant shape. *SIAM J. Math. Anal.* **15**, 723–736 (1984).

**Supplementary Information** is linked to the online version of the paper at [www.nature.com/nature](http://www.nature.com/nature).

**Acknowledgements** I thank J. Fischer and M. Kirkpatrick for their comments on the manuscript.

**Author Information** Reprints and permissions information is available at [www.nature.com/reprints](http://www.nature.com/reprints). Correspondence and requests for materials should be addressed to T.H.K. (tkeitt@mail.utexas.edu).

## METHODS

**Wavelet analysis.** The LRL data were collected roughly every 2 weeks in warmer months and approximately every 6 weeks in winter. Irregular sampling precludes standard numerical methods based on the fast Fourier transform. Instead, I directly computed the inner product of the data samples and the scaled and translated wavelet function. The zero-padded signal for each species is given by

$$x_k(\tau) = \sum_i \delta(\tau - v_i) x_k(v_i) \quad (3)$$

where  $v_i$  is the time of the  $i$ th sample and  $\delta(\cdot)$  is the delta function. Substitution in equation (1) yields

$$w_k(t, s) = s^{-1} \sum_i \psi\left(\frac{t - v_i}{s}\right) x_k(v_i) \quad (4)$$

where the equivalence holds under relatively weak smoothness and continuity conditions for  $x$  and  $s$  at or above the Nyquist scale<sup>13</sup>. I approximate the Nyquist scale as twice the mean time lag between samples and require  $s$  to be at least 1.5 times this value. Equation (4) was evaluated at regular intervals separated by the average time lag between successive LRL sampling dates (21 days) and  $s$  ranged from 2 months to 5 years.

**Wavelet modulus ratios and phases.** The wavelet modulus ratio can be estimated locally (equation (2)) or accumulated over the entire time series. The global case is given by

$$\rho(s) = \frac{\langle |\sum_k w_k(t, s)| \rangle}{\langle \sum_k |w_k(t, s)| \rangle} \quad (5)$$

where  $\langle \cdot \rangle$  denotes the arithmetic mean with respect to time (see margin plots in Fig. 1). Wavelet phase was computed as  $\theta = \tan^{-1}\left(\frac{a}{b}\right)$  where  $a$  and  $b$  are real and imaginary parts of the wavelet coefficient. Annual-scale phase differences were rescaled to months and further adjusted to sidestep the December to January discontinuity<sup>24</sup> using the formula  $\frac{6}{\pi} [(\Delta\theta + 3\pi) \text{ modulo } 2\pi] - 6$ .

**Null model simulation via stochastic wavelets.** A common approach to estimating a null distribution based on independent fluctuations is repeated shuffling of individual species time series<sup>4,27</sup>. Time series randomization alters serial correlations and can drastically alter the underlying null model such that estimated probabilities are biased relative to the ideal null model where species fluctuate independently, but all other properties of the original time series are preserved<sup>28</sup>. To overcome this obstacle, I developed an alternative method where random perturbations are introduced to the wavelet and the original time series remain intact. The stochastic wavelets, indexed by species and scale, are given by

$$\psi_{k,s}(\tau) = \pi^{-1/4} \exp\left(2\pi i\left[\tau + \varepsilon_{k,s}\right] - \frac{1}{2}\tau^2\right) \quad (6)$$

where  $\varepsilon_{k,s}$  are uniform samples from the interval  $(-1/2, 1/2)$ . The perturbation is equivalent to a simple phase shift in the wavelet domain for each species at each scale. Null distributions were estimated from 1,000 independent trials. I controlled the false discovery rate at the 5% level using the method previously described<sup>29</sup>, which is valid in the presence of interdependence. Application of the phase-perturbation method to simulated data indicates high statistical power and low bias in the presence of zeros in time series data (Supplementary Figs 2 and 3).

27. Ernest, S. K. M. & Brown, J. H. Homeostasis and compensation: the role of species and resources in ecosystem stability. *Ecology* **82**, 2118–2132 (2001).

28. Solow, A. & Duplisea, D. Testing for compensation in a multi-species community. *Ecosystems* **10**, 1034–1038 (2007).

29. Benjamini, Y. & Yekutieli, D. The control of the false discovery rate in multiple testing under dependency. *Ann. Statist.* **29**, 1165–1188 (2001).